THE PENNSYLVANIA STATE UNIVERSITY
SCHREYER HONORS COLLEGE

DEPARTMENT OF COMPUTER SCIENCE AND ENGINEERING

THE DISCRETE CURVELET TRANSFORM FOR QUANTUM ALGORITHMS

JUSTIN T. KEREKES
Spring 2010

A thesis
submitted in partial fulfillment
of the requirements
for baccalaureate degrees
in Computer Science and Mathematics
with honors in Computer Science

Reviewed and approved* by the following:

Sean Hallgren
Assistant Professor
Thesis Supervisor

John Hannan
Associate Professor
Honors Adviser

* Signatures are on file in the Schreyer Honors College.

Abstract

This thesis explores the possibility of using the discrete quantum curvelet transform on square functions in two dimensions for use in different quantum algorithms such as Yi-Kai Liu's center finding algorithm. I verify that using the discrete curvelet transform on a uniform quantum state in two dimensions will yield a new quantum state with a better-than-uniform probability to measure the corners of the distribution.

Acknowledgment

I want to express my gratitude to my thesis adviser, Professor Sean Hallgren, for his time, patience, enthusiasm, and all of the different topics he explored with me throughout my junior and senior years.

TABLE OF CONTENTS

Abstract i
Table of Contents ii

Chapter 1. INTRODUCTION 1

Chapter 2. BACKGROUND INFORMATION 2
Chapter 3. ASSESSING THE PROBLEM..... 6
Chapter 4. USING THE QUANTUM CURVELET 10
TRANSFORM IN ONE DIMENSION
Chapter 5. USINE THE QUANTUM CURVELET..... 22
TRANSFORM IN TWO DIMENSIONS
Chapter 6. CONCLUSIONS AND FUTURE WORK 27

Bibliography..... 29

1. Introduction

We have known for over a decade that quantum computers can run algorithms that significantly outperform classical computation, as exemplified by Peter Shor's integer factorization algorithm that runs in polynomial time and space [2]. One of the major goals of studying quantum computation is to understand which computational problems can be solved faster with quantum algorithms than classical algorithms.

The number of classical algorithms greatly exceeds the number of quantum algorithms in general. The same is true in the case of algorithms using the curvelet transform, as there are many classical uses for the curvelet transform, such as image compression [5] and removing noise from images [6]. Therefore, the possibility that the quantum curvelet transform can be used in quantum algorithms motivates us to look for such algorithms.

The point of this thesis is to help to find another way in which the quantum curvelet is actually useful. Yi-Kai Liu devised several algorithms that use the quantum curvelet transform (center finding for a radial function, single-shot measurement of a quantum-sample state)[1], and he conjectures that his discrete algorithms succeed with constant probability, independent of the dimension, by imitating the continuous curvelet transform. This thesis moves toward a way to analyze square uniform distributions and how the quantum curvelet transform acts on them. If there exists a way to rigorously prove that the discrete curvelet transform has the same properties as the continuous curvelet transform using square functions, then perhaps the same results could be applied to radial functions. These findings would verify the validity of Yi-Kai Liu's conjectures.

We present a starting point for approaching the problem of determining the likeness between quantum and continuous curvelet transforms. Instead of looking at all uniform distributions in general, we simplify the problem to a two-dimensional square distribution. However, even a simple square distribution requires us to first analyze a simpler distribution, the one-dimensional uniform distribution.

First we will analyze some of the properties of the quantum curvelet transform acting on a one-dimensional uniform distribution. Then we will apply our analysis to the square uniform distribution in two dimensions. Finally we will compare the likeness of the discrete versus continuous curvelet transforms.

2. Background Information

We will start with the necessary foundations of quantum computation. While classical computation uses bits, quantum computation's most fundamental concept is the quantum bit, or qubit. A qubit's state is generally represented in Dirac notation which looks like $|0\rangle$. While a classical bit is either a zero or a one, a qubit can be any of $|0\rangle$, $|1\rangle$, or a superposition of both $|0\rangle$ and $|1\rangle$. When a qubit is a superposition of the two basis states, it is unknown whether measuring the qubit would yield a $|0\rangle$ or a $|1\rangle$. Examples of superpositions of quantum states are

$$|\gamma_1\rangle = a_1|0\rangle + b_1|1\rangle$$
$$|\gamma_2\rangle = |0\rangle$$
$$|\gamma_3\rangle = a_3|00\rangle + b_3|01\rangle + c_3|10\rangle + d_3|11\rangle \quad This\ system\ has\ 2\ qubits$$

$|\gamma_1\rangle$ and $|\gamma_3\rangle$ are formed by taking a linear combination of quantum states. The coefficients, $a_1, b_1, a_3, b_3, c_3, and\ d_3$, are all complex valued. We can think about $|\gamma_1\rangle$ as a vector in a two-dimensional vector space whose basis vectors are $|0\rangle$ and $|1\rangle$. Then $|\gamma_3\rangle$ is a vector in a four-dimensional vector space, and its basis vectors are $|00\rangle$, $|01\rangle$, $|10\rangle$, $|11\rangle$.

We can represent a quantum system as the superposition of quantum states by

$$c_0|x_0\rangle + c_1|x_1\rangle + \cdots + c_{N-1}|x_{N-1}\rangle = \sum_{i=0}^{N-1} c_i|x_i\rangle$$

The Hilbert space associated with this system is the complex vector space, and each of the states $|x_0\rangle, |x_1\rangle, \ldots, |x_{N-1}\rangle$ are its basis vectors. The state of this system is represented by a unit-length vector in the Hilbert space, thus the sum of the squares of the coefficients must be equal to one.

$$\sum_{i=0}^{N-1} |c_i|^2 = 1$$

When we measure a qubit, $|\gamma\rangle = a|0\rangle + b|1\rangle$, we will see either $|0\rangle$ or $|1\rangle$, but not both. We will measure $|0\rangle$ with probability $|a|^2$, and we will measure $|1\rangle$ with probability $|b|^2$. Thus it makes sense that the sum of the squares of the probabilities must be 1. When we measure a quantum superposition, $\sum_{i=0}^{N-1} c_i|x_i\rangle$, we are given the following relationship between the probability of

measuring a particular state in the system and the coefficient associated with that basis state in the system.

$$P(Measure\ x_i) = |c_i|^2$$

The superposition $\sum_{i=0}^{N-1} c_i|x_i\rangle$ makes up a unit vector in an N-dimensional complex vector space which is called a Hilbert space. Some examples of unit vectors in this system are

$$|\gamma\rangle = \frac{1}{\sqrt{3}}|0\rangle + \frac{1}{\sqrt{3}}|1\rangle + \frac{1}{\sqrt{3}}|2\rangle \qquad N = 3$$

$$|\varphi\rangle = \frac{1}{2}|0\rangle + \frac{1}{2}|1\rangle - \frac{1}{2}|2\rangle - \frac{1}{2}|3\rangle \qquad N = 4$$

Classical circuits work by passing classical bits through wires and logic gates. Analogously, quantum circuits work by passing quantum information through quantum gates. Therefore, quantum computation will involve sending data through possibly many different quantum gates. Conveniently, we can express quantum gates in matrix form. For example, taking a single qubit, $|\gamma\rangle = a|0\rangle + b|1\rangle$ and writing it in vector form looks like $|\gamma\rangle = a\begin{bmatrix}1\\0\end{bmatrix} + b\begin{bmatrix}0\\1\end{bmatrix}$. Now we apply the NOT quantum gate by multiplying $|\gamma\rangle$ by $A_{NOT} = \begin{bmatrix}0 & 1\\1 & 0\end{bmatrix}$.

$$\begin{aligned} A_{NOT}|\gamma\rangle &= aA_{NOT}\begin{bmatrix}1\\0\end{bmatrix} + bA_{NOT}\begin{bmatrix}0\\1\end{bmatrix} \\ &= a\begin{bmatrix}0 & 1\\1 & 0\end{bmatrix}\begin{bmatrix}1\\0\end{bmatrix} + b\begin{bmatrix}0 & 1\\1 & 0\end{bmatrix}\begin{bmatrix}0\\1\end{bmatrix} \\ &= b\begin{bmatrix}1\\0\end{bmatrix} + a\begin{bmatrix}0\\1\end{bmatrix} \\ &= b|0\rangle + a|1\rangle \end{aligned}$$

As we have shown, applying the NOT gate to a qubit swaps the coefficients associated with the quantum states $|0\rangle$ and $|1\rangle$. Instead of representing the NOT gate with a matrix, we can simply say that it takes the state $|1\rangle$ to the state $|0\rangle$ and the state $|0\rangle$ to the state $|1\rangle$.

There are many different useful quantum gates. The only requirement for a quantum gate to work on a qubit is that the matrix U describing the quantum gate must be unitary. The matrix U is unitary if $VU = I$, where I is the identity matrix, and V is the adjoint of U. We can find the adjoint by

taking the transpose followed by the complex conjugate of U. The new state vector will still be a unit vector.

The analysis in this thesis requires us to understand the quantum curvelet transform. We define the quantum curvelet transform in terms of two quantum gates, the Fourier transform and the inverse Fourier Transform.

The discrete Fourier transform is as follows. For an integer a in which $0 \leq a < N$ where N is the size of the Hilbert space (the number of basis states), the discrete Fourier transform is the unitary operation takes the state $|a\rangle$ to the state

$$\frac{1}{\sqrt{N}} \sum_{x=0}^{N-1} \exp\left(\frac{2\pi i a x}{N}\right) |x\rangle$$

We will not be using matrix notation in this thesis, however the matrix form of the Fourier transform can be found in Michael Nielsen and Isaac Chuang's book listed in the references chapter [8]. The inverse discrete Fourier transform is also a unitary operation, and it takes the state $|a\rangle$ to the state

$$\frac{1}{\sqrt{N}} \sum_{x=0}^{N-1} \exp\left(\frac{-2\pi i a x}{N}\right) |x\rangle$$

The quantum curvelet transform is the unitary operation that maps:

$$\sum_{\vec{x}} f(\vec{x})|\vec{x}\rangle|0,\vec{0}\rangle \quad \xrightarrow{Curvelet\ \ Transform} \quad \sum_{a,\vec{b},\vec{\theta}} \gamma_f(a,\vec{b},\vec{\theta})\ |\vec{b}\rangle|a,\vec{\theta}\rangle$$

Where both functions are defined on finite domains, $0 < a < 1$ is the scale (the smaller this value, the finer the scale), $\vec{b} \in \mathbb{R}^n$ is a location, and $\vec{\theta} \in S^{n-1}$ (the unit sphere in $\mathbb{R}^n$) is a vector that we use for a direction. We accomplish the curvelet transform by (1) applying the Fourier transform on $f(\vec{x})$ to get $\hat{f}(\vec{x})$, (2) applying a *window function* (explained in Chapter 4) that separates $\hat{f}(\vec{x})$ into different subspaces, and (3) taking the inverse Fourier transform.

When analyzing expressions with complex exponents, it is helpful to recall Euler's formula: $For\ any\ real\ number\ x,\ \ e^{ix} = \cos(x) + i * sin(x)$ where *e* is the base of the natural logarithm, and *i* is the imaginary unit.

When measuring the norm (or absolute value) of a complex number, we use the following formula:

$$|ai + b| = \sqrt{a^2 + b^2}$$

3. Assessing the Problem

As mentioned in the introduction, Yi-Kai Liu developed several algorithms using the quantum curvelet transform. However, he conjectured the validity of his algorithms by comparing the quantum (discrete) curvelet transform to the continuous curvelet transform [1]. He argues that for a fine enough scale, the discrete curvelet transform looks more and more like the continuous one, so for a large enough Hilbert space, the discrete curvelet transform should work for his quantum algorithms. We set out to prove more rigorously that the discrete curvelet transform works as intended for a large enough Hilbert space.

One of the major characteristics of the continuous curvelet transform is that after we apply it to a uniform distribution in n dimensions, the probability density becomes more concentrated near the edges of the distribution. For example, in two dimensions a uniform distribution looks like a rectangle. After applying the continuous curvelet transform, the probability of measuring the edges or corners increases significantly, while the probability of measuring the center of the shape approaches zero.

The other important characteristic of the continuous curvelet transform that we would like to show is that the transform returns a relevant direction as well. The direction is essential for Liu's center finding algorithms that involve using the returned direction to point towards the center of the distribution. We will leave the direction vector out of the analysis and include its details in Chapter 6.

Before attempting to prove the properties of the quantum curvelet transform, we needed data that would suggest that we could get a reasonable lower bound for measuring the edges of a uniform distribution over some shape. In my 2-dimensional analysis, I focus on a square-shaped distribution. If the analysis for the square shape yields positive results, then we could have a starting point which could lead our analysis of distributions with other shapes. Also, if the analysis in one and two dimensions showed reasonably large lower bounds on the probability densities near the edges of the uniform distribution, then perhaps that would help lead to a proof for the n-dimensional case.

First we focused on the one-dimensional case. In one dimension, a uniform distribution from $|a\rangle$ to $|b\rangle$ means we have a quantum system where the probability of measuring $|a\rangle, |b\rangle,$ and everything in

between is $\frac{1}{b-a+1}$, but the probability of measuring everything else is 0. Using MATLAB, I computed the curvelet transform of this distribution using different values for a, b, and N. Then I calculated the probability of measuring $|a\rangle$ and $|b\rangle$ for each case and looked for patterns.

I noticed that the probabilities of $|a\rangle$ and $|b\rangle$ were equal for all of my test cases. This was good news because it suggests some degree of symmetry. For this reason, I will continue refer to the probability of measuring $|a\rangle$ instead of both $|a\rangle$ and $|b\rangle$ with the understanding that the probability of measuring$|b\rangle$ acts the same as the probability of measuring $|a\rangle$.

An interesting fact that we learned by running experimental test cases is that regardless of the values of $|a\rangle$ and $|b\rangle$, we would always get the probabilities if $(b-a)$ stayed the same. Thus, if $a = 5\ and\ b = 10$ then the probability of measuring $|a\rangle$ and $|b\rangle$ is the same as the probability of measuring$|a\rangle$ and $|b\rangle$ if $a = 22\ and\ b = 27$. Therefore, it does not matter where in space the uniform distribution sits, only the size of the distribution. We were able to prove this; however I left out the proof because it is not relevant to the goals of this thesis.

Another immediate observation on the experimental data is that the probability of measuring $|a\rangle$ starts high if the distribution is small, but as the distribution becomes wider, the probability of measuring the endpoints decreases. If we let $s \coloneqq b - a + 1$, the experimental data shows a negative correlation between s and the probability of measuring $|a\rangle$.

Although the probability of measuring $|a\rangle$ decreases as s increases, there is a probability spike around $|a\rangle$ and $|b\rangle$ regardless of how high s is (see Figure 1). The goal in analyzing the distribution is to find a lower bound on this spike (showing that the probability must be at least some value) and show that the probability is better than uniform.

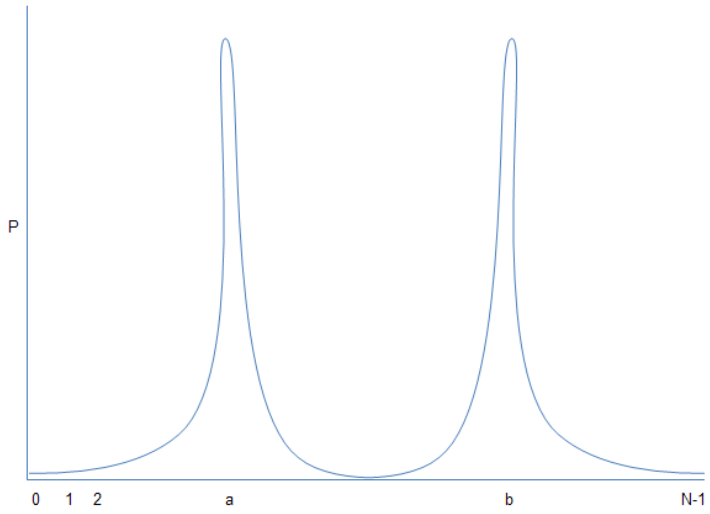

Figure 1: The probability spikes around a and b after the curvelet transform

Looking at Figure 1, we can see that if N gets really big, then the probability density will be distributed over more values, so we would normally expect the probability of measuring $|a\rangle$ to decrease. This idea is contrary to what actually happens. As N increases, the probability of measuring $|a\rangle$ increases and slowly converges to some value, suggesting that the probability of measuring values far from $|a\rangle$ and $|b\rangle$ get smaller and smaller as N increases. This observation is consistent with Yi-Kai Liu's suggestion that using finer scales (increasing N) causes the discrete curvelet transform to act more like the continuous curvelet transform.

These observations suggest that finding a significant lower bound independent of N might be possible in one dimension. However, applying these findings in higher dimensions presents its own set of obstacles. When defining the curvelet transform in Chapter 2, we mentioned the use of a window function. The window function can be one of many different functions from which we can choose ourselves. Different window functions can influence the probability analysis, making it easier or more difficult.

In the one-dimensional analysis, we use a power-of-two window function where each window is twice the size of the window that came before it. This means the last window takes up exactly half the space, and it is relatively easier to analyze than many other window functions. However, when we adopt this approach in two dimensions, the last window using power-of-two windows only takes up one quarter of the space, instead of one half. While it is still a relatively easy window to analyze, its impact is less significant because it takes up a smaller fraction of the space.

We set out to prove a bound that will be asymptotically greater than uniform $\left(\frac{1}{s^n}\right)$ with the hope of achieving a lower bound of around $O\left(\frac{1}{s}\right)$ regardless of dimension because that would validate everything in Yi-Kai Liu's algorithms except the analysis of the direction vector returned by the discrete curvelet transform. But first we need to start simple. We have data to suggest we can find a better-than-uniform bound for measuring the edges in one dimension, so Chapter 4 seeks to prove such a bound. Then in Chapter 5, we try to extend this bound to the two dimensional case and see why it might not scale well.

4. Using the Quantum Curvelet Transform in One Dimension

We start with a quantum superposition over a uniform distribution from $|a\rangle\ to\ |b\rangle$ in a size N Hilbert space. The state vector is a unit vector, so the sum of the squares of the coefficients equals one. Therefore, we are required to include a *normalization factor* in front of each of the quantum states, $\frac{1}{\sqrt{b-a+1}}$.

$$|\varphi\rangle = \frac{1}{\sqrt{b-a+1}}|a\rangle + \frac{1}{\sqrt{b-a+1}}|a+1\rangle + \cdots + \frac{1}{\sqrt{b-a+1}}|b\rangle = \frac{1}{\sqrt{b-a+1}}\sum_{x=a}^{b}|x\rangle$$

In Chapter 2, we laid out the steps to applying the quantum curvelet transform. First we need to apply a Fourier transform, then the windowing function, and finally the inverse Fourier transform. The Fourier transform and inverse Fourier transform are both unitary operations, so after they are applied, the sum of the squares of the coefficients must still be one. That is why there is an extra factor of $\frac{1}{\sqrt{N}}$ in the formulas for the Fourier and inverse Fourier transforms. We are going to apply the discrete Fourier transform to the system that we already have.

$$Let\ \omega \coloneqq e^{\frac{2\pi i}{N}}$$

$$\frac{1}{\sqrt{b-a+1}}\sum_{x=a}^{b}|x\rangle \quad \xrightarrow{Fourier\ \ Transform} \quad \frac{1}{\sqrt{N}\sqrt{b-a+1}}\sum_{y=0}^{N-1}\sum_{x=a}^{b}\omega^{xy}\,|y\rangle$$

After we apply the Fourier transform to a function, we say that it is no longer in its time domain, but its frequency domain. Had we applied the Fourier transform and then the inverse Fourier transform without any intermediate steps, we would have ended up with the same uniform distribution that we started with. To get meaningful results using the curvelet transform, we need to separate the function in the frequency domain into different subspaces before applying the inverse Fourier transform.

To view only pieces of the function in the frequency domain, we apply an indicator function known as a *window function*. This window function "zeroes out" part of the superposition that does not lie within the window's bounds (See Figure 2). We also add a new register, $|w\rangle$, which isolates each of these windows into their own subspaces.

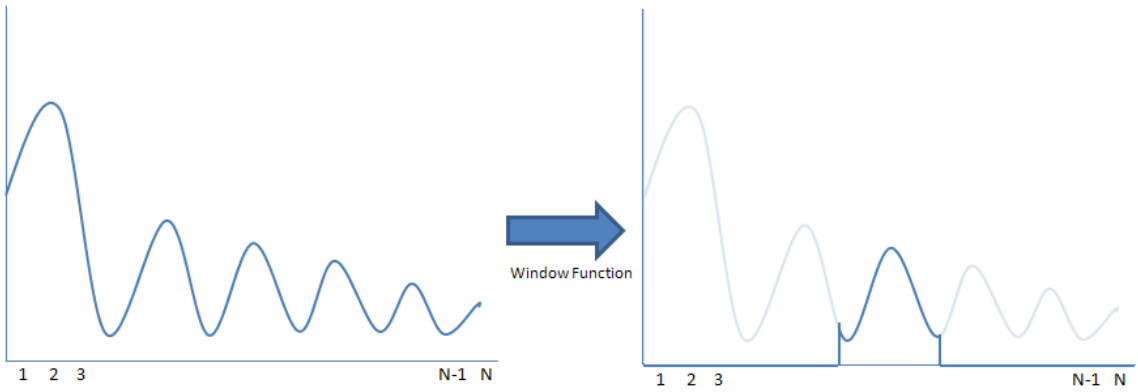

Figure 2: Applying the window function "zeros out" the distribution everywhere outside of each window.

Once we separate the system into different subspaces, the system becomes the superposition over all of the windows. As mentioned earlier, there are many different ways to define window functions, and they each grant us different algebraic properties [3].

The type of windows we are going to use will be powers of two. Each window will be twice as large as the last (we assume N is a power of 2 for simplicity). Other possible constructions for the window function are given in Emmanuel Candés' papers [3, 4]. The window function that we will apply is

$$g_w(y) = \begin{cases} 1 & if\ 2^{w-1} \le y < 2^w \\ 0 & otherwise \end{cases}$$

We want to be able to measure a value in a particular window, so we are going to add a register, w, and sum over all of the windows. This allows us to avoid renormalizing the system and accomplishes the "zeroing out" by putting different parts of the superposition into different subspaces.

$$\frac{1}{\sqrt{N}\sqrt{b-a+1}} \sum_{w=1}^{\log_2 N} \sum_{y=0}^{N-1} \sum_{x=a}^{b} \omega^{xy}\ g_w(y)|y\rangle\,|w\rangle$$

The window register indicates in which window each value falls. The window function simply splits up our space into windows of size 2^w, for $w \coloneqq 1, 2, \dots, \log N$, so that we can measure on each window individually. Finally, we apply the inverse discrete Fourier transform to get

$$\frac{1}{N}\frac{1}{\sqrt{b-a+1}} \sum_{z=0}^{N-1} \sum_{w=1}^{\log_2 N} \sum_{y=0}^{N-1} \sum_{x=a}^{b} \omega^{xy}\ \omega^{-zy}\, g_w(y)|z\rangle\,|w\rangle$$

At this point we have performed all of the steps of the curvelet transform, and the above expression is what we are left with. Because the continuous curvelet transform causes the probability of measuring the endpoints of distributions to be high, we expect the same behavior from the discrete curvelet transform, and we will seek to prove that next. We want to lower bound the probability of measuring $|a\rangle \; or \; |b\rangle$ after applying the quantum curvelet transform, and we are hoping to find a bound that is better than uniform.

The probability of measuring $|a\rangle$ is complicated because we have to take into account all windows that can each contribute some probability of measuring $|a\rangle$ to find the actual probability. However, we are only interested in a lower bound for now, so we do not have to find the probability of measuring $|a\rangle$ for each window. Instead, we can lower bound the probability of measuring $|a\rangle$ over all windows by the probability of measuring $|a\rangle$ over a particular window.

Claim 4.0: If $P_w(a)$ is the probability of measuring $|a\rangle$ *and* window $|w\rangle$, and $P(a)$ is the probability of measuring $|a\rangle$, then $P_w(a) \leq P(a)$.

Proof:

The probability of measuring $|a\rangle$ is the probability of measuring $|a\rangle$ for each window, which can be expressed as a summation.

$$P(a) = \sum_{w=1}^{\log N} P_w(a)$$

Since all probabilities must be positive, it follows that $P_w(a) \leq P(a)$ for any particular window, w.

We mentioned in Chapter 3 that our experimental data led us to believe that the probability of measuring both endpoints is the same, and this observation made the distribution seem symmetric. We know that the distribution cannot be completely symmetric because $|a\rangle \; and \; |b\rangle$ are generally not centered at $\frac{N}{2}$, however the peaks of the probability distribution at $|a\rangle \; and \; |b\rangle$ always have the same height experimentally.

Claim 4.1: $P_{w_0}(a) = P_{w_0}(b)$ for any window w_0, where *a* is the lower bound of the distribution in one dimension, and *b* is the upper bound.

Proof:

In a quantum system, the probability of measuring a particular state is equal to the square of the norm of the coefficient of that state. The system we have is shown below.

$$\frac{1}{N}\frac{1}{\sqrt{b-a+1}}\sum_{z=0}^{N-1}\sum_{w=1}^{\log_2 N}\sum_{y=0}^{N-1}\sum_{x=a}^{b}\omega^{xy}\,\omega^{-zy}\,g_w(y)|z\rangle\,|w\rangle$$

If we want to find only the probability of measuring $|a\rangle|w_0\rangle$, we need to simplify this summation. To find the coefficient of $|a\rangle|w_0\rangle$, we simply set $z = a$ and remove the summation over z. Also, we set $w = w_0$ and remove the summation over w. Everything that is left is the coefficient of $|a\rangle|w_0\rangle$. Then the probability is the square of the norm of the coefficient in front of $|a\rangle|w_0\rangle$. Then by definition

$$P_{w_0}(a) = \left|\frac{1}{N}\frac{1}{\sqrt{b-a+1}}\sum_{y=0}^{N-1}\sum_{x=a}^{b}\omega^{xy}\,\omega^{-ay}g_{w_0}(y)\right|^2$$

$$P_{w_0}(b) = \left|\frac{1}{N}\frac{1}{\sqrt{b-a+1}}\sum_{y=0}^{N-1}\sum_{x=a}^{b}\omega^{xy}\,\omega^{-by}g_{w_0}(y)\right|^2$$

Therefore, it is sufficient to show that $\left|\sum_{y=0}^{N-1}\sum_{x=a}^{b}\omega^{xy}\,\omega^{-ay}g_{w_0}(y)\right| = \left|\sum_{y=0}^{N-1}\sum_{x=a}^{b}\omega^{xy}\,\omega^{-by}g_{w_0}(y)\right|$, and that would imply that $P_{w_0}(a) = P_{w_0}(b)$.

$$\left|\sum_{y=0}^{N-1}\sum_{x=a}^{b}\omega^{-ay+xy}\,g_{w_0}(y)\right| = \left|\sum_{y=0}^{N-1}[\omega^0 g_w(y) + \omega^y g_w(y) + \cdots + \omega^{by-ay}\,g_{w_0}(y)]\right|$$

$$= \left|\sum_{y=0}^{N-1} g_{w_0}(y)\left[1 + e^{\frac{2\pi yi}{N}} + \cdots + e^{\frac{2\pi(by-ay)i}{N}}\right]\right|$$

$$= \left|\sum_{y=0}^{N-1} g_{w_0}(y)\,\left[1 + \cos\left(\frac{2\pi y}{N}\right) + isin\left(\frac{2\pi y}{N}\right) + \cdots + \cos\left(\frac{2\pi(by-ay)}{N}\right) + \text{isin}\left(\frac{2\pi(by-ay)}{N}\right)\right]\right|$$

$$= \sqrt{\left(\sum_{y=0}^{N-1} g_{w_0}(y)\left(1 + \cos\left(\frac{2\pi y}{N}\right) + \cdots + \cos\left(\frac{2\pi(by-ay)}{N}\right)\right)\right)^2 + \left(\sum_{y=0}^{N-1} g_{w_0}(y)\left(sin\left(\frac{2\pi y}{N}\right) + \cdots + \sin\left(\frac{2\pi(by-ay)}{N}\right)\right)\right)^2}$$

$$= \sqrt{\left(\sum_{y=0}^{N-1} g_{w_0}(y)\left(1 + \cos\left(-\frac{2\pi y}{N}\right) + \cdots + \cos\left(\frac{2\pi(ay-by)}{N}\right)\right)\right)^2 + \left((-1)\sum_{y=0}^{N-1} g_{w_0}(y)\left(sin\left(\frac{2\pi y}{N}\right) + \cdots + \sin\left(\frac{2\pi(by-ay)}{N}\right)\right)\right)^2}$$

$$= \sqrt{\left(\sum_{y=0}^{N-1} g_{w_0}(y)\left(1+\cos\left(-\frac{2\pi y}{N}\right)+\cdots+\cos\left(\frac{2\pi(ay-by)}{N}\right)\right)\right)^2+\left(\sum_{y=0}^{N-1} g_{w_0}(y)\left(sin\left(-\frac{2\pi y}{N}\right)+\cdots+\sin\left(\frac{2\pi(ay-by)}{N}\right)\right)\right)^2}$$

$$= \left|\sum_{y=0}^{N-1} g_{w_0}(y)\left[1+\cos\left(-\frac{2\pi y}{N}\right)+isin\left(-\frac{2\pi y}{N}\right)+\cdots+\cos\left(\frac{2\pi(ay-by)}{N}\right)+\text{isin}\left(\frac{2\pi(ay-by)}{N}\right)\right]\right|$$

$$= \left|\sum_{y=0}^{N-1} g_{w_0}(y)\left[1+e^{\frac{-2\pi yi}{N}}+\cdots+e^{\frac{2\pi(ay-by)i}{N}}\right]\right|$$

$$= \left|\sum_{y=0}^{N-1} g_{w_0}(y)[\omega^0+\omega^{-y}+\cdots+\omega^{ay-by}]\right| = \left|\sum_{y=0}^{N-1}\sum_{x=a}^{b}\omega^{-by+xy}\, g_{w_0}(y)\right|$$

Thus $\left|\sum_{y=0}^{N-1}\sum_{x=a}^{b}\omega^{-ay+xy}\, g_{w_0}(y)\right| = \left|\sum_{y=0}^{N-1}\sum_{x=a}^{b}\omega^{-by+xy}\, g_{w_0}(y)\right|$ which implies $P_{w_0}(a) = P_{w_0}(b)$, and this concludes the proof.

Using Claim 4.1, we know that in order to find a lower bound for P(a) and P(b), it is sufficient to find a lower bound for just P(a). Using Claim 4.0, in order to find a lower bound for P(a), it is sufficient to find a lower bound for $P_{w_0}(a)$ for some window w_0. Therefore, to show a lower bound for the probability of measuring $|a\rangle\ and\ |b\rangle$, we only need to show a lower bound for the probability of measuring $|a\rangle$ on one particular window. We will continue this chapter by only analyzing the very last window. This window contains exactly half of the summation terms by the way we constructed the window function.

$P_{final}(a) = \left|\frac{1}{N}\frac{1}{\sqrt{b-a+1}}\sum_{y=1}^{N}\sum_{x=a}^{b}\omega^{xy}\,\omega^{-ay}\, g_w(y)\right|^2$, but we know that $g_w(y)$ restricts this to only the y values after $\frac{N}{2}$ since we are using the final window, w. Therefore, we can eliminate the indicator function because we know it equals one for all y values such that $\frac{N}{2} \le y < N-1$, and it equals zero everywhere else.

$$P_{final}(measure\ a) = \left|\frac{1}{N}\frac{1}{\sqrt{b-a+1}}\sum_{y=0}^{N-1}\sum_{x=a}^{b}\omega^{xy}\,\omega^{-ay}\, g_{final}(y)\right|^2$$

$$= \left|\frac{1}{N}\frac{1}{\sqrt{b-a+1}}\sum_{y=\frac{N}{2}}^{N-1}\sum_{x=a}^{b}\omega^{-ay+xy}\right|^2$$

$$= \frac{1}{N^2(b-a+1)}\left|\sum_{x=a}^{b}\sum_{y=\frac{N}{2}}^{N-1}\omega^{-ay+xy}\right|^2$$

This is a very tricky double summation because every omega term adds a complex-valued sine and cosine function that may not add together very easily. To be able to analyze this probability, we need to be able to reduce these omega terms into values that add together more easily. We found the following way to reduce the inner summation into a simpler form.

Claim 4.2: The following formula can be used to reduce summations of omega terms.

$$\sum_{y=\frac{N}{2}}^{N-1} \omega^{-Cy} = \begin{cases} 0 & if\ C\ \neq 0\ is\ even \\ i * cot\frac{C\pi}{N} - 1 & if\ C\ is\ odd \end{cases}$$

Proof:

Case exponent, C, is even: C = 2k for some $k \in Z \neq 0$

$$\sum_{y=\frac{N}{2}}^{N-1} \omega^{-2ky} = \omega^{-2k\left(\frac{N}{2}\right)} + \omega^{-2k\left(\frac{N}{2}+1\right)} + \omega^{-2k\left(\frac{N}{2}+2\right)} + \cdots + \omega^{-2kN+2k}$$

$$= \omega^{-Nk}[\omega^0 + \omega^{-2k} + \omega^{-4k} + \cdots + \omega^{-Nk+2k}]$$

$$= \omega^{-Nk}\left(\frac{\omega^{-Nk}-1}{\omega^{-2k}-1}\right) = \frac{\omega^{-2kN} - \omega^{-kN}}{\omega^{-2k}-1}$$

$$= \frac{e^{-4\pi ki} - e^{-2\pi ki}}{e^{\frac{-4\pi ki}{N}} - 1}$$

$$= \frac{cos(4\pi k) - isin(4\pi k) - cos(2\pi k) + isin(2\pi k)}{cos\left(\frac{4\pi k}{N}\right) - isin\left(\frac{4\pi k}{N}\right) - 1} = 0$$

This verifies the top half of the piecewise function.

Case exponent is odd: C = 2k+1 for some $k \in Z$

$$\sum_{y=\frac{N}{2}}^{N-1} \omega^{-2ky-y} = \omega^{-(2k+1)\left(\frac{N}{2}\right)} + \omega^{-(2k+1)\left(\frac{N}{2}+1\right)} + \omega^{-(2k+1)\left(\frac{N}{2}+2\right)} + \cdots + \omega^{-2kN-N+2k+1}$$

$$= \omega^{-N\left(k+\frac{1}{2}\right)}\left[\omega^0 + \omega^{-2k-1} + \omega^{-4k-2} + \cdots + \omega^{-N\left(k+\frac{1}{2}\right)+(2k+1)}\right]$$

$$= \omega^{-kN-\frac{N}{2}}\left[\frac{\omega^{-kN-\frac{N}{2}}-1}{\omega^{-2k-1}-1}\right] = \frac{\omega^{-2kN-N} - \omega^{-kN-\frac{N}{2}}}{\omega^{-2k-1}-1}$$

$$= \frac{\omega^{-2kN-N+2k+1} - \omega^{-kN-\frac{N}{2}+2k+1}}{1-\omega^{2k+1}}$$

$$= \frac{e^{-4\pi ki-2\pi i+\frac{4\pi ki+2\pi i}{N}} - e^{-2\pi ki-\pi i+\frac{4\pi ki+2\pi i}{N}}}{1-e^{\frac{4\pi ki+2\pi i}{N}}}$$

The following two identities follow from the fact that sine and cosine are 2π-periodic:

(1) $e^{-4\pi ki-2\pi i+\frac{4\pi ki+2\pi i}{N}} = e^{\frac{4\pi ki+2\pi i}{N}}$

(2) $e^{-2\pi ki-\pi i+\frac{4\pi ki+2\pi i}{N}} = e^{\pi i+\frac{4\pi ki+2\pi i}{N}}$

$$Let\ L \coloneqq \frac{4\pi k+2\pi}{N}, then$$

$$\frac{e^{-4\pi ki-2\pi i+\frac{4\pi ki+2\pi i}{N}} - e^{-2\pi ki-\pi i+\frac{4\pi ki+2\pi i}{N}}}{1-e^{\frac{4\pi ki+2\pi i}{N}}} = \frac{e^{Li} - e^{\pi i+Li}}{1-e^{Li}}$$

$$= \frac{\cos(L) + isin(L) - \cos(L+\pi) - isin(L+\pi)}{1-\cos(L)-isin(L)}$$

Next we are going to use the following basic trigonometric identities to help us reduce the quotient.

$$\cos(x+\pi) = -\cos(x) \quad and \quad \sin(x+\pi) = -\sin(x)$$

$$\frac{e^{Li} - e^{\pi i+Li}}{1-e^{Li}} = \frac{2\cos(L) + 2isin(L)}{1-\cos(L)-isin(L)}$$

$$= \frac{2(\cos(L) + isin(L)(1-\cos(L)+isin(L))}{\big(1-\cos(L)-isin(L)\big)(1-\cos(L)+isin(L))}$$

$$= \frac{2\big(-cos^2(L) - sin^2(L) + \cos(L) + isin(L)\big)}{cos^2(L) + sin^2(L) - 2\cos(L) + 1}$$

$$= \frac{-1+\cos(L)+isin(L)}{1-\cos(L)}$$

$$= \frac{isin(L)}{1-\cos(L)} - 1$$

$$= \frac{i\sin^2(L)}{(\sin(L))(1-\cos(L))} - 1$$

$$= \frac{i(1-\cos(L)(1+\cos(L))}{(\sin(L))(1-\cos(L))} - 1$$

$$= i\big(csc(L) + cot(L)\big) - 1$$

$$= i * csc(L) + i * cot(L) - 1$$

$$= i * cot\left(\frac{L}{2}\right) - 1$$

$$= i * cot\left(\frac{C\pi}{N}\right) - 1$$

This concludes the proof of Claim 4.2, the simplification of the omega summation.

When calculating the norm, we need to be able to separate the real and imaginary parts. Reducing the omega terms this way is very convenient because it separates the real and imaginary parts without requiring any extra work. Applying the results of Claim 4.2, we can simplify the double summation.

$$\begin{aligned}\sum_{x=a}^{b}\sum_{y=\frac{N}{2}}^{N-1}\omega^{-ay+xy} &= \sum_{y=\frac{N}{2}}^{N-1}\sum_{x=a}^{b}\omega^{-ay+xy}\\ &= \sum_{y=\frac{N}{2}}^{N-1}[\omega^{0}+\omega^{y}+\omega^{3y}+\cdots+\omega^{\left\lceil\frac{b-a}{2}\right\rceil y}]\\ &= \sum_{C=0}^{\left\lceil\frac{b-a}{2}\right\rceil}\left[i*cot\left(\frac{(2C+1)\pi}{N}\right)-1\right]\\ &= -\left\lceil\frac{b-a+2}{2}\right\rceil+i*\sum_{C=0}^{\left\lceil\frac{b-a}{2}\right\rceil}cot\left(\frac{(2C+1)\pi}{N}\right)\end{aligned}$$

The first term is approximately $-\frac{b-a+2}{2}$, but summing over the rest of the terms which include a cotangent function is fairly challenging. To lower bound the summation, I used the notion that the integral of a function translates to the area under its curve. If I view each term in the cotangent summation as a rectangle that also takes up some area, I can show that the area of the integral is less than or equal to the area of the summing rectangles. This is the basic idea behind the next claim.

Claim 4.3: $\sum_{C=0}^{\left\lceil\frac{b-a}{2}\right\rceil}cot\left(\frac{(2C+1)\pi}{N}\right)\geq\int_{0}^{\left\lceil\frac{b-a}{2}\right\rceil}cot\left(\frac{(2C+1)\pi}{N}\right)dC$

Proof:

When we look at the graph for the cotangent function (Figure 3), we notice that it is completely symmetric, and all values on the left side of the symmetry are positive. Therefore, if $\left\lceil\frac{a-b}{2}\right\rceil\ll\frac{N}{4}$, we know that all terms in the summation are positive, and we know that the integral is always positive.

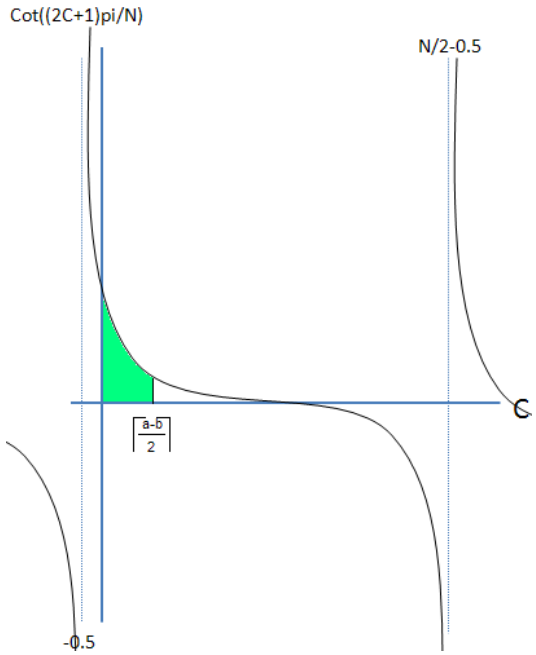

Figure 3: The shaded region represents the area returned by the integral

When we look at the graph of cotangent with rectangles over top of where the summation terms are (Figure 4), we see that each rectangle has a width of one, so the sum of all the terms in the summation equals the combined area of the rectangles. The area covered by the summation must be at least the area covered by the integral.

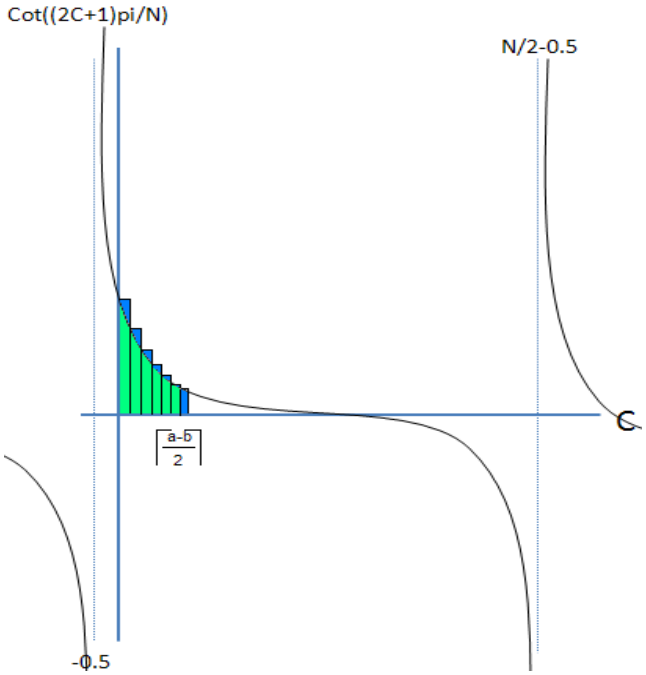

Figure 4: The green is covered by the integral and the summation, while the blue is only covered by the summation.

According to the graphs shown, there is no way to cover more area with the integral than with the

summation, since the section of the graph we are interested in is always positive and always decreasing. This concludes our proof that: $\sum_{C=0}^{\left\lceil\frac{b-a}{2}\right\rceil} cot\left(\frac{(2C+1)\pi}{N}\right) \geq \int_{0}^{\left\lceil\frac{b-a}{2}\right\rceil} cot\left(\frac{(2C+1)\pi}{N}\right) dC$

It is helpful to note here that $\int cot\left(\frac{(2C+1)\pi}{N}\right) dC = \frac{N}{2\pi} \ln\left|\sin\left(\frac{2\pi C+\pi}{N}\right)\right|$. We can easily verify this by taking the derivative with respect to C.

At this point, we have enough simplification of the terms to be able to lower bound the probability of measuring $|a\rangle$ on the final window. We will combine all real terms and imaginary terms, take the norm, and analyze the behavior as N approaches ∞.

Claim 4.4: For sufficiently large N with respect to $s \coloneqq b - a + 1$, $P_{final}\,(a)$ is bounded below by

$$\frac{\pi^2 + ln^2(s+1)}{4\pi^2 s}$$

Proof:

As before, P_{final} refers to the probability of measuring some value only on the last window. Using Claim 4.1, we find the probability of measuring $|a\rangle$ on the final window by using the probability of measuring $|b\rangle$ on the final window.

$$P_{final}\,(a) = P_{final}\,(b)$$

$$= \frac{1}{N^2(b-a+1)} \left| \sum_{x=a}^{b} \sum_{y=\frac{N}{2}}^{N-1} \omega^{-by+xy} \right|^2$$

We want to simplify the terms, so that we can understand more easily the behavior of this formula.

Let $s \coloneqq b - a + 1$

$$P_{final}\,(a) = \frac{1}{N^2 s} \left| \sum_{y=\frac{N}{2}}^{N-1} \left(1 + \omega^{-y} + \omega^{-2y} + \cdots + \omega^{(a-b)y}\right) \right|^2$$

$$= \frac{1}{N^2 s} \left| \frac{N}{2} + \sum_{y=\frac{N}{2}}^{N-1} \left(\omega^{-y} + \omega^{-2y} + \cdots + \omega^{(a-b)y}\right) \right|^2$$

Here we can use Claim 4.2 to turn the omega terms into complex terms that involve the cotangent function.

$$\frac{1}{N^2 s}\left|\frac{N}{2}+\sum_{y=\frac{N}{2}}^{N-1}\left(\omega^{-y}+\omega^{-2y}+\cdots+\omega^{(a-b)y}\right)\right|^2 = \frac{1}{N^2 s}\left|\frac{N}{2}+\sum_{C=0}^{\left\lfloor\frac{b-a}{2}\right\rfloor}\left(i*cot\left(\frac{(2C+1)\pi}{N}\right)-1\right)\right|^2$$

$$= \frac{1}{4N^2 s}\left|N-(b-a+1)+2\sum_{C=0}^{\left\lfloor\frac{b-a}{2}\right\rfloor}\left(i*cot\left(\frac{(2C+1)\pi}{N}\right)\right)\right|^2$$

We approximated $\left\lceil\frac{b-a}{2}+1\right\rceil \approx \frac{b-a}{2}+1$ which will only be off by at most one. To eliminate fractions, we also pulled a factor of $\frac{1}{2}$ out of the squared norm. Calculating the norm involves separating the real parts from the separate parts and following the formula for finding the absolute value of a complex number.

$$\left|N-s+2i*\sum_{C=0}^{\frac{s}{2}}cot\left(\frac{(2C+1)\pi}{N}\right)\right|^2 = (Real\ Part)^2+(Imaginary\ Part)^2$$

$$= (N-s)^2+4\left(\sum_{C=0}^{\frac{s}{2}}cot\left(\frac{(2C+1)\pi}{N}\right)\right)^2$$

$$= N^2-2Ns+s^2+4\left(\sum_{C=0}^{\frac{s}{2}}cot\left(\frac{(2C+1)\pi}{N}\right)\right)^2$$

Using Claim 4.3, we can lower bound the summation of each cotangent term by the integral of the cotangent term.

$$N^2-2Ns+s^2+4\left(\sum_{C=0}^{\left\lceil\frac{s}{2}\right\rceil}cot\left(\frac{(2C+1)\pi}{N}\right)\right)^2 \geq N^2-2Ns+s^2+4\left(\int_0^{\left\lceil\frac{s}{2}\right\rceil}cot\left(\frac{(2C+1)\pi}{N}\right)dC\right)^2$$

$$\int_0^{\left\lceil\frac{s}{2}\right\rceil}cot\left(\frac{(2C+1)\pi}{N}\right)dC = \frac{N}{2\pi}\ln\left|\sin\left(\frac{2\pi\left\lceil\frac{s}{2}\right\rceil+\pi}{N}\right)\right|-\frac{N}{2\pi}\ln\left|\sin\left(\frac{\pi}{N}\right)\right|$$

$$= \frac{N}{2\pi}\left(\ln\left|\sin\left(\frac{2\pi\left\lceil\frac{s}{2}\right\rceil+\pi}{N}\right)\right|-\ln\left|\sin\left(\frac{\pi}{N}\right)\right|\right)$$

Since we are assuming that $s \ll N$ and that N is very large, we can approximate very accurately:

$$\frac{N}{2\pi}\left(\ln\left|\sin\left(\frac{2\pi\left\lceil\frac{s}{2}\right\rceil+\pi}{N}\right)\right|-\ln\left|\sin\left(\frac{\pi}{N}\right)\right|\right) \approx \frac{N}{2\pi}\left(\ln\frac{2\pi\left\lceil\frac{s}{2}\right\rceil+\pi}{N}-\ln\frac{\pi}{N}\right)$$

$$\frac{N}{2\pi}\left(\ln\frac{2\pi\left\lceil\frac{s}{2}\right\rceil+\pi}{N}-\ln\frac{\pi}{N}\right)\approx\frac{N}{2\pi}\ln(s+1)$$

Thus for large $N \gg s$,

$$P_{final}\,(a) \geq \frac{1}{4N^2 s}\left(N^2-2Ns+s^2+4\left(\frac{N}{2\pi}\ln(s+1)\right)^2\right)=\frac{1}{4s}-\frac{1}{2N}+\frac{s}{N^2}+\frac{ln^2(s+1)}{4\pi^2 s}$$

When $N \gg s$, two terms disappear and we are left with:

$$P_{final}\,(measure\ a) \geq \frac{\pi^2+ln^2(s+1)}{4\pi^2 s}=O\left(\frac{ln^2(s)}{s}\right)$$

If we assume s to be a constant, then we can say that the probability has a constant lower bound for any sufficiently large N. By Claim 4.1 we know that the probability of measuring b in the final window shares the same lower bound. Also, by Claim 4.0, we know that the probability of measuring a and b for any window is lower bounded by $P_{final}\,(measure\ a)$.

Immediately we can see that the probability of measuring an endpoint is going to be greater than the probability of measuring the same endpoint uniformly from $b-a$ points provided that $b-a$ is sufficiently less than N. This is typical of the curvelet transform in general. The probability for most shapes (we have a square here) should be denser near the edges. We are going to need this analysis of the 1-dimensional case in order to analyze the 2-dimensional case.

5. Using the Quantum Curvelet Transform in Two Dimensions

Again we start with a quantum superposition over a uniform distribution from $|a,a\rangle \; to \; |b,b\rangle$ in a size N^2 Hilbert space.

$$|\varphi\rangle = \frac{1}{b-a+1}|a,a\rangle + \frac{1}{b-a+1}|a+1,a\rangle + \frac{1}{b-a+1}|a+1,a+1\rangle + \cdots + \frac{1}{b-a+1}|b,b\rangle$$

$$= \frac{1}{b-a+1}\sum_{y=a}^{b}\sum_{x=a}^{b}|x,y\rangle$$

We are going to go through the same steps of the quantum curvelet transform as we did in the one-dimensional case. First we apply the Fourier transform, followed by a window function, and finally the inverse Fourier transform.

$$Let\ \omega \coloneqq e^{\frac{2\pi i}{N}}$$

$$\frac{1}{b-a+1}\sum_{y=a}^{b}\sum_{x=a}^{b}|x,y\rangle \quad \xrightarrow{Fourier\ \ Transform} \quad \frac{1}{N(b-a+1)}\sum_{j=0}^{N-1}\sum_{y=a}^{b}\sum_{k=0}^{N-1}\sum_{x=a}^{b}\omega^{xk}\,\omega^{yj}\;|x,y\rangle$$

Once again, we are going to "zero out" part of the distribution at this point by separating it into pieces and moving the pieces into different subspaces. To do so we are going to apply a window function. The choice of window function is up to us. We do not have to use powers of two, although in this analysis we will.

$$g_{w_1,w_2}(j,k) = \begin{cases} 1 & if\ 2^{w_1-1} \le j < 2^{w_1}\ and\ 2^{w_2-1}\ k < 2^{w_2} \\ 0 & otherwise \end{cases}$$

After applying the window function, our summation looks like this:

$$\frac{1}{N(b-a+1)}\sum_{w_1=1}^{\log N}\sum_{w_2=1}^{\log N}\sum_{j=0}^{N-1}\sum_{y=a}^{b}\sum_{k=0}^{N-1}\sum_{x=a}^{b}\omega^{xk}\,\omega^{yj}\,g_{w_1,w_2}(j,k)\,|x,y\rangle$$

In Euclidean space, the upper-right fourth of our $N\ x\ N$ grid makes up the very last window, $w_1 = w_2 = log_2 N$. Figure 5 shows how the window setup looks in two dimensions.

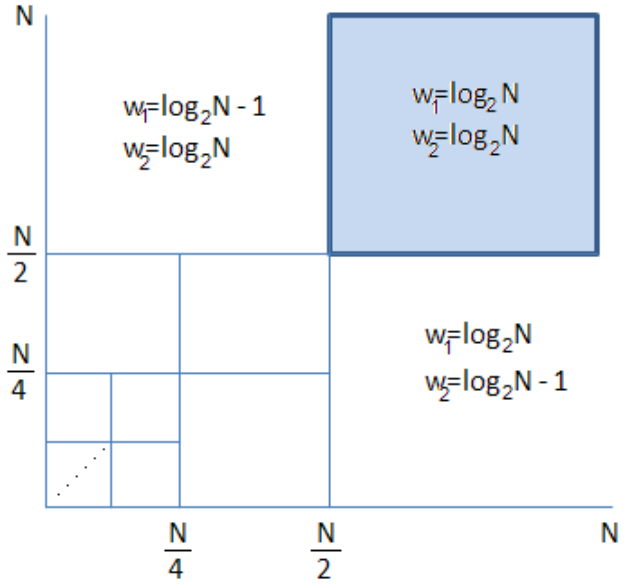

Figure 5: The last window is the upper-right hand corner, and it represents a fourth of all of the summation terms.

After applying the window function, we apply the inverse Fourier transform to complete the curvelet transform.

$$\frac{1}{N(b-a+1)} \sum_{w_1=1}^{\log N} \sum_{w_2=1}^{\log N} \sum_{j=0}^{N-1} \sum_{y=a}^{b} \sum_{k=0}^{N-1} \sum_{x=a}^{b} \omega^{xk}\, \omega^{yj}\, g_{w_1,w_2}(j,k)\, |x, y, \vec{w}\rangle$$

$$\xrightarrow[Inverse\ \ Fourier\ \ Transform]{}$$

$$\frac{1}{N^2(b-a+1)} \sum_{z_1=0}^{N-1} \sum_{z_2=0}^{N-1} \sum_{w_1=1}^{\log N} \sum_{w_2=1}^{\log N} \sum_{j=0}^{N-1} \sum_{y=a}^{b} \sum_{k=0}^{N-1} \sum_{x=a}^{b} \omega^{xk+yj}\, \omega^{-z_1 j - z_2 k}\, g_{w_1,w_2}(j,k)\, |z_1, z_2, \vec{w}\rangle$$

Instead of trying to bound the probability of the edge as in the 1-dimensional case, we are now interested in bounding the probability of measuring a corner.

Claim 5.0: When measuring on the final window ($w_1 = w_2 = log_2 N$),

$$P\big(measure\ (a,a)\big) = P\big(measure\ (b,b)\big)$$

Proof:

We want to measure the corner (a, a) in the last window. To find the probability of measuring (a, a) in the last window, we take the square of the norm of the coefficient of $|a, a, w_1 = \log N, w_2 = \log N\rangle$. Since we are no longer summing over z_1 and z_2, we can remove those two summations. Also, we

are no longer summing over w_1 and w_2, so we can also eliminate those two summations. What we are left with is

$$P_{last}\,(measure\ a, a) = \left| \frac{1}{N^2(b-a+1)} \sum_{j=0}^{N-1} \sum_{y=a}^{b} \sum_{k=0}^{N-1} \sum_{x=a}^{b} \omega^{xk+yj}\, \omega^{-aj-ak}\, g_{w_1,w_2}(j,k) \right|^2$$

But we know that in the last window, $g_{w_1,w_2}(j,k) = 0$ unless $\frac{N}{2} \leq j,k < N$ in which case $g_{w_1,w_2}(j,k) = 1$.

$$P_{last}\,(measure\ a, a) = \left| \frac{1}{N^2(b-a+1)} \sum_{j=\frac{N}{2}}^{N-1} \sum_{y=a}^{b} \sum_{k=\frac{N}{2}}^{N-1} \sum_{x=a}^{b} \omega^{xk+yj}\, \omega^{-aj-ak} \right|^2$$

We can get the probability to look like what it did in the one-dimensional case.

$$\left| \frac{1}{N^2(b-a+1)} \sum_{j=\frac{N}{2}}^{N-1} \sum_{y=a}^{b} \sum_{k=\frac{N}{2}}^{N-1} \sum_{x=a}^{b} \omega^{xk+yj}\, \omega^{-aj-ak} \right|^2$$

$$= \frac{1}{N^4(b-a+1)^2} \left| \sum_{j=\frac{N}{2}}^{N-1} \sum_{y=a}^{b} \sum_{k=\frac{N}{2}}^{N-1} \sum_{x=a}^{b} \omega^{xk+yj}\, \omega^{-aj-ak} \right|^2$$

$$= \frac{1}{N^4(b-a+1)^2} \left| \sum_{j=\frac{N}{2}}^{N-1} \sum_{y=a}^{b} \omega^{-aj+yj} \sum_{k=\frac{N}{2}}^{N-1} \sum_{x=a}^{b} \omega^{-ak+xk} \right|^2$$

$$= \frac{1}{N^4(b-a+1)^2} \left| \left(\sum_{j=\frac{N}{2}}^{N-1} \sum_{y=a}^{b} \omega^{-aj+yj} \right)^2 \right|^2$$

From the proof of Claim 4.1, we have the following equality.

$$\left| \sum_{j=\frac{N}{2}}^{N-1} \sum_{y=a}^{b} \omega^{-aj+yj} \right| = \left| \sum_{j=\frac{N}{2}}^{N-1} \sum_{y=a}^{b} \omega^{-bj+yj} \right|$$

Using this equality, we can manipulate the terms inside the norm to eventually become the probability of measuring (b, b) on the last window.

$$P_{last}\,(measure\ a,a) = \frac{1}{N^4(b-a+1)^2}\left|\left(\sum_{j=\frac{N}{2}}^{N-1}\sum_{y=a}^{b}\omega^{-aj+yj}\right)^2\right|^2 = \frac{1}{N^4(b-a+1)^2}\left|\left(\sum_{j=\frac{N}{2}}^{N-1}\sum_{y=a}^{b}\omega^{-bj+yj}\right)^2\right|^2$$
$$= P_{last}\,(measure\ b,b)$$

This concludes the proof of Claim 5.0, that the probability of measuring the bottom-left and top-right corners of the square created by $(a,a) to\ (b,b)$ is the same.

Claim 5.1: For sufficiently large N with respect to s, $P_{final}\,(measure\ a,a)$ is bounded below by

$$\left(\frac{\pi^2+ln^2(s+1)}{4\pi^2 s}\right)^2$$

Proof:

By Claim 5.0, we can replace the probability of measuring (a,a) with the probability of measuring (b,b). Also, we can combine the exponent of the summation with the exponent of the norm.

$$P_{last}\,(a,a) = \frac{1}{N^4 s^2}\left|\left(\sum_{j=\frac{N}{2}}^{N-1}\sum_{y=a}^{b}\omega^{-aj+yj}\right)^2\right|^2$$
$$= P_{last}\,(measure\ b,b)$$
$$= \frac{1}{N^4 s^2}\left|\left(\sum_{j=\frac{N}{2}}^{N-1}\sum_{y=a}^{b}\omega^{-bj+yj}\right)\right|^4$$

We can manipulate the summation to make the terms resemble the terms in the one-dimensional analysis.

$$\sum_{y=a}^{b}\omega^{-bj+yj} = \omega^{aj-bj} + \omega^{aj-bj+j} + \cdots + \omega^{-j} + \omega^{0} = \sum_{y=a}^{b}\omega^{aj-yj}$$

$$P_{last}\,(b,b) = \left(\frac{1}{N^2 s}\left|\sum_{j=\frac{N}{2}}^{N-1}\sum_{y=a}^{b}\omega^{aj-yj}\right|^2\right)^2$$

By Claim 4.4, this is bounded below for sufficiently large $N \gg s$ by $\left(\frac{\pi^2+ln^2(s)}{4\pi^2(s)}\right)^2$. This concludes the proof of Claim 5.1.

The probability of measuring one of the two corners (a, a) or (b, b) is $O\left(\frac{ln^2(s)}{s}\right)$ and independent of N. Immediately it is clear that the probability of measuring the upper-right or lower-left corner is better than in a uniform distribution, however without measuring over all of the windows and summing the probability, we cannot tell if the probability of measuring a corner on any window will be constant. This proof can be extended to n-dimensional shapes as well, where the two corners are the one closest to the origin and the one farthest from the origin. In general the probability of measuring one of these corners on the last window is $O\left(\left(\frac{ln^2(b-a)}{b-a}\right)^n\right)$. We could prove this the same way we proved the lower bound in the two dimensional case.

6. Conclusions and Future Work

We know for sure that in the closest and farthest corners from the origin, the probability density spikes. We can easily see that $\left(\frac{ln^2(s)}{s}\right)^n = \omega\left(\frac{1}{s^n}\right)$, so we achieve asymptotically better-than-uniform probability on the corners of the square.

One major drawback to the analysis performed in this thesis is that the lower bound probability for measuring a corner on the last window, $O\left(\left(\frac{ln^2(s)}{s}\right)^n\right)$, does not scale well at all in higher dimensions. This is mostly because the "last window" is an exponentially small fraction $\frac{1}{2^n}$ of the N^n Hilbert space. Yi-Kai Liu's algorithms that use the quantum Fourier transform are very scalable. He conjectures that his algorithms work with constant probability in terms of the dimension [1]. We have only provided a starting point for being able to prove whether or not we can achieve constant probability in terms of the dimension.

We use the powers-of-two window definition in the 2-dimensional case because it is convenient to analyze. When we calculate the probability of measuring $|a\rangle$ and $|b\rangle$ using the powers-of-two windows, there is much almost no deconstructive interference. This suggests that it is a relatively good window function to use to maximize probabilities. Since we did not prove otherwise, it is possible that the way that we defined the windows in this analysis does yield a scalable lower bound. We only analyzed the probability of the "last window". Perhaps if we would sum over all of the windows, we would get a more scalable bound. Understanding the summation over all windows in the 2-dimensional analysis would require us to simplify six summations which may not reduce to something as simple as a cotangent function.

If we could prove that we cannot get a scalable lower bound for the powers-of-two window function, perhaps a different choice of window function could yield a scalable lower bound. Yi-Kai Liu uses polar coordinates for his window functions, so it makes more sense for his windows to cut up space into a more spherical shape. His windows are essentially slices of a pie that become more numerous as N increases. Analyzing this choice of window function for the quantum curvelet transform could give more concrete results that scale well.

We are missing one key component in this analysis that prevents us from applying it to Liu's center finding algorithms. The curvelet transform is known to be a "directional" transform that returns both a location and a direction upon measuring. Yi-Kai Liu's algorithms rely on the direction returned to be able to find the center of the inputted radial function or the center of a sphere. The direction returned is given by the window that is measured, therefore to determine what the probability distribution looks like for the directional vector, we need to analyze the probability distribution of measuring a particular window. Because Yi-Kai Liu uses radial functions and windows that resemble pie slices, he can get a fairly precise direction returned. Because we use square window functions that get larger as they get farther from the origin, we are very limited to the number of vectors that the direction could be. I conjecture that the powers-of-two definition of windows will inhibit us from getting an accurate directional vector with any useful probability. It would be useful to prove such results.

References

[1] Liu, Yi-Kai. Quantum Algorithms Using the Curvelet Transform. Institute for Quantum Information. California Institute of Technology, March 25, 2009.

[2] Shor, Peter W. Polynomial-Time Algorithms for Prime Factorization and Discrete Logarithms on a Quantum Computer. Society for Industrial and Applied Mathematics. SIAM J. COMPUT., Vol. 26, No. 5:1494-1509, 1997.

[3] Candés, Emmanuel, Laurent Demanet, David Donoho, and Lexing Ying. Fast Discrete Curvelet Transforms. Applied and Computational Mathematics, California Institute of Technology, 2005.

[4] Ying, Lexing, Laurent Demanet, and Emmanuel Candés. 3D Discrete Curvelet Transform. Applied and Computational Mathematics, California Institute of Technology, 2005.

[5] Joshi, M. S., R. R. Manthalkar, and Y. V. Joshi. Image Compression Using Curvelet, Ridgelet and Wavelet Transform, A Comparative Study. ICGST-GVIP, Vol. 8, No. 3, 2008.

[6] Sivakumar, R. Denoising of Computer Tomography Images Using Curvelet Transform. ARPN Journal of Engineering and Applied Sciences, Vol. 2, No. 1, 2007.

[7] Grover, Lov and Terry Rudolph. Creating Superpositions that Correspond to Efficiently Integrable Probability Distributions. Bell Labs. 2008

[8] Nielsen, Michael and Isaac Chuang. Quantum Computation and Quantum Information. Cambridge University Press. 216-221. 2007

ACADEMIC VITA of Justin T. Kerekes

Justin T. Kerekes
P.O. Box 187
1627 Swamp Pike
Gilbertsville, PA 19525
jok5076@psu.edu

Education:

Bachelor of Science Degree in Computer Science,
Penn State University, Spring 2010
Bachelor of Science Degree in Mathematics,
Penn State University, Spring 2010
Minor in Spanish
Honors in Computer Science
Thesis Title: The Discrete Curvelet Transform for Quantum Algorithms
Thesis Supervisor: Dr. Sean Hallgren

Related Experience:

Summer REU at Penn State University
Supervisor: Dr. Sean Hallgren
Sponsered by NSF
Summer 2010

Grading Assistant for Data Structures and Algorithms
Penn State University: Department of Computer Science and Engineering
Fall 2009

Awards:

President's Freshman Award
Lockheed Martin Engineering Scholars' Award
Dean's List

Activities:

Mission work in Guatemala, Puerto Rico, and Peru
Treasurer of Alliance Christian Fellowship
Member of the National Society of Collegiate Scholars